On the Nth roots of -1 and complex basin boundaries : fractals from Newton-Raphson

Christian, JM and Middleton-Spencer, HAJ

http://dx.doi.org/10.1080/07468342.2020.1703452

Title	On the Nth roots of -1 and complex basin boundaries : fractals from Newton-Raphson
Authors	Christian, JM and Middleton-Spencer, HAJ
Type	Article
URL	This version is available at: http://usir.salford.ac.uk/id/eprint/56536/
Published Date	2020

USIR is a digital collection of the research output of the University of Salford. Where copyright permits, full text material held in the repository is made freely available online and can be read, downloaded and copied for non-commercial private study or research purposes. Please check the manuscript for any further copyright restrictions.

For more information, including our policy and submission procedure, please contact the Repository Team at: usir@salford.ac.uk.

On the Nth Roots of -1 and Complex Basin Boundaries: Fractals from Newton-Raphson

J. M. Christian and H. A. J. Middleton-Spencer

James Christian (j.christian@salford.ac.uk) is a lecturer in the Joule Physics Laboratory at the University of Salford, UK. His current research interests include various theoretical problems in electromagnetics, classical fluids, and nonlinear waves. When not writing papers or teaching, he spends an unhealthy amount of time tinkering with fractals just for the fun of it.

Holly Middleton-Spencer (h.a.j.middleton-spencer2@newcastle.ac.uk) is a PhD student of applied mathematics at the University of Newcastle, UK, studying matter wave solitons in expanding Bose-Einstein condensates. She is formerly a student at the University of Salford, where James was the supervisor for her MSc degree on electromagnetic scattering from fractal screens.

Can you find the roots of a quadratic equation? It is not a trick question, but nor is it quite so straightforward as one might imagine. While many readers can no doubt recite the famous formula, committed to memory since high school days, that is not quite what we mean here. Let us consider the roots of $f_2(z) := z^2 + 1 = 0$. The two answers are evidently $z = +i$ and $z = -i$, where $i := \sqrt{-1}$ is the imaginary unit. Throughout this article, we shall represent complex numbers such as $z = x + iy$ in the Argand plane (with the real part, x, on the horizontal axis and the imaginary part, y, on the vertical axis).

One may instead choose to attack the problem on computer, regarding our opening question as an exercise (albeit a seemingly trivial one) in numerical root-finding. In that case, an off-the-shelf iterative algorithm for which many of us would probably reach first is the Newton-Raphson (N-R) method [1]. Plugging the function $f_2(z)$ into the standard formula $z_{n+1} = z_n - f_2(z_n)/f_2'(z_n)$, with the prime denoting derivative with respect to z, we arrive at a simple feedback loop:

$$z_{n+1} = z_n - \frac{z_n^2 + 1}{2z_n}. \tag{1}$$

The discrete subscript index $n = 1, 2, 3, \ldots$ labels successive iterations—hopefully tending towards a more accurate answer—and with z_0 representing a first guess at a root. Supplying such an initial condition is always necessary in order to get the N-R algorithm started off. We might now write a basic computer code to obtain the 'output' (interpreted quite generally as the collection of numbers $\{z_n\}$ for $n = 1, 2, 3, ..$) systematically for a whole range of different 'inputs' (taken to be z_0 values). With $z_0 := x_0 + iy_0$ suitably specified, a not unreasonable expectation is that $z_n = x_n + iy_n$ converges to either root, $z = \pm i$, as $n \to \infty$. In practice, one considers not the limit but
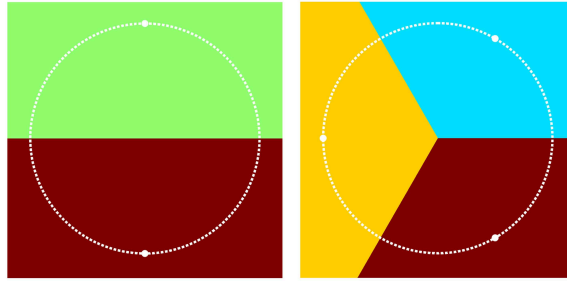
Figure 1. Section of the (x_0, y_0) Argand plane of initial conditions with position of the roots denoted by solid white circles and the dotted white line showing the unit circle. Left: Iterations of Eq. (1) tend to $z = +i$ (located in the upper half-plane) when z_0 lies in the green region, or to $z = -i$ (located in the lower half-plane) when z_0 is in the red region. Right: A schematic diagram showing the expectation for the iterations of Eq. (3), prior to any number-crunching.

rather finite n sufficiently large that $|z_{n+1} - z_n|$ is below some desired tolerance. With luck, only a handful of iterations will be necessary.

Surprises in a quadratic

By color-coding the outcome of each calculation, the Argand plane of initial conditions, (x_0, y_0), is neatly broken up into two distinct regions by the straight line $y_0 = 0$ [see Fig. 1(left)]. Initial conditions with $y_0 > 0$ lead to iterates $z_1, z_2, z_3, ...$ that wander around in the plane, as prescribed by Eq. (1), and converge on $z = +i$; those with $y_0 < 0$ converge on $z = -i$ in the same sort of way. That is not a very interesting result, but it is quite instructive to bear in mind for what follows. It also serves as a portent for how even apparently simple systems can sometimes catch us all by surprise [2].

The square-roots problem is usually treated very briefly (if at all) and solely as a precursor to the much more exciting case of finding the cube roots of -1. But it is worth paying attention to square roots for just a little longer. Suppose we separate Eq. (1) into its real and imaginary parts so that

$$x_{n+1} = \frac{(x_n^2 + y_n^2) - 1}{2 (x_n^2 + y_n^2)} x_n, \tag{2a}$$

$$y_{n+1} = \frac{(x_n^2 + y_n^2) + 1}{2 (x_n^2 + y_n^2)} y_n. \tag{2b}$$

An initial condition with $y_0 = 0$ is lying on the *geometrical boundary* between the roots, and from Eq. (2b) it now becomes obvious that $y_n = 0$ for $n = 1, 2, 3, ...$. The iterates must thus stay forever trapped on the real axis and the solution cannot converge on either of the roots $z = \pm i$ (located on the imaginary axis). We may also consider what happens to x_n by setting $y_n = 0$ in Eq. (2a), which leads to

$$x_{n+1} = \frac{x_n^2 - 1}{2x_n}. \tag{2c}$$

For any arbitrary x_0, the iterates jump to and fro along the x axis and often seem to behave rather erratically: plotting x_n against n, the solution typically *looks random*. It
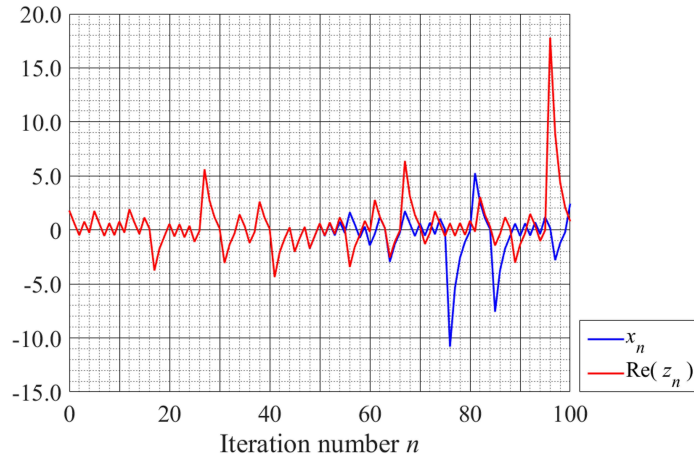
Figure 2. Comparison of the iterates of Eq. (2c) with an initial condition $x_0 = 1.8$ (blue line) with those from Eq. (1) when $z_0 = 1.8 + i0$ (red line). The solutions are more or less identical until $n \approx 50$, at which point they begin to separate and diverge. Closer inspection shows that $|x_3 - \text{Re}(z_3)| \approx 10^{-16}$, $|x_{20} - \text{Re}(z_{20})| \approx 10^{-11}$, $|x_{40} - \text{Re}(z_{40})| \approx 10^{-5}$, and $|x_{50} - \text{Re}(z_{50})| \approx 0.02$.

is, of course, not random at all since Eq. (2c) is a purely deterministic rule [2]. Even more curiously, we soon find that there emerges a difference between the solution predicted by Eq. (2c) and that obtained from Eq. (1) when using the entirely equivalent initial condition $z_0 = x_0 + i0$ (see Fig. 2). We will return to this point later on.

From quadratics to cubics

Consider now the cubic equation $f_3(z) := z^3 + 1 = 0$. After a bit of algebra, we find that the three roots are $\exp(i\pi/3)$, $\exp(i\pi)$, and $\exp(i5\pi/3)$. Moreover, we know they form an equilateral triangle and that they must lie on the circumference of a unit circle centred on the origin of the Argand plane. For the function $f_3(z)$, the N-R iterates are governed by

$$z_{n+1} = z_n - \frac{z_n^3 + 1}{3z_n^2}. \tag{3}$$

Using the *square roots of −1* as a guide, it feels intuitive that the (x_0, y_0) plane should be divided into three equally-sized wedges. Moreover, the geometrical boundary between those regions may well be defined by straight lines described by angles relative to the x_0 axis of $\theta = 0$, $\theta = 2\pi/3$ and $\theta = 4\pi/3$ [see Fig. 1(right)]. Hopefully, the iterations from Eq. (3) will converge on one of the roots for any given z_0, and we can again color-code which root ultimately 'wins'. From our knowledge of how the square roots behave, we might also modify the earlier code to introduce a fourth color accommodating the possibility of *no convergence*, just in case the algorithm fails to give us a reasonable answer for some z_0 values [3,4].
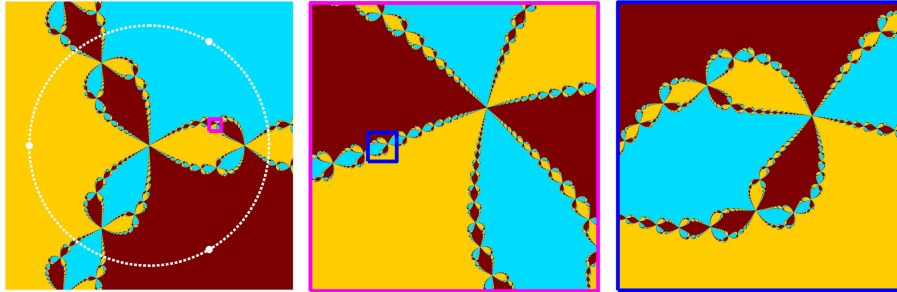
Figure 3. Basins of attraction obtained by iterating Eq. (3). The panes consider the regions $-1.2 \leq (x_0, y_0) \leq 1.2$ (left), $0.5 \leq x_0 \leq 0.6$ and $0.12 \leq y_0 \leq 0.22$ (middle, where the square domain has side 0.1) and $0.52 \leq x_0 \leq 0.53$ and $0.165 \leq y_0 \leq 0.175$ (right, where the square domain has side 0.01).

Complex boundaries

As discovered by John Hubbard in the 1970s [5], the Argand plane does not break up in such a straightforward way for the cube-roots problem. The basic expectation of having 'three separate wedges' survives, but the boundaries between those regions are most definitely not straight lines. They are far more complex: beautifully intricate patterns that become objects of mathematical interest in their own right and rendering the original root-finding considerations purely secondary. The boundaries—which resemble a 'string of pearls'—appear to have the property of being *fractal*. That is, they retain comparable levels of detail under arbitrary magnifications (see Fig. 3). An alternative interpretation is that a fractal has no natural scalelength (or, equivalently, *all possible scalelengths*).

With the unexpected emergence of these patterns in mind, it is helpful to reinterpret the iterative scheme of Eq. (3) as prescribing discrete motion in a two-dimensional map (readily obtained, after a little bit of algebra, by isolating the real and imaginary parts). Viewed through the modern prism of dynamical systems [1], the three roots we found analytically for Eq. (3) may be thought of as *fixed-point attractors* in a 'lossy' system—that is to say, three isolated points towards which (x_n, y_n) *trajectories*, bouncing around the in the (x, y) plane as n increases, are simultaneously pulled.

In Fig. 3, the set of all initial conditions whose subsequent trajectories converge toward $\exp(i\pi/3)$ is shown in turquoise (those sets for $\exp(i\pi)$ and $\exp(i5\pi/3)$ are in yellow and red, respectively). The turquoise region is referred to as the *basin of attraction* for the attractor at $\exp(i\pi/3)$, with similar descriptions for the other two colors and roots [6]. The boundaries between the three principal wedges have some intriguing properties. For instance, the string-of-pearls evidently persists across three decimal orders of scale, but it shows no sign of disappearing under further magnifications. One also cannot move from a region of turquoise into a region of red without crossing a region of yellow (or, more subtly, into and out of yellow regions an infinite number of times). Similar is true for all other permutations of colors, and this mind-bending characteristic is what topologists call the Wada property [7].

While Fig. 3 shows the basins for the *cube roots of* −1, it is pertinent to note that the patterns are necessarily identical in form to those obtained when considering the similar *cube roots of* +1 problem instead. The basins for these two closely-related systems are connected by a rotation because the geometrical boundaries are always determined relative to the position of the roots. In switching between "−1" and "+1" variants, the
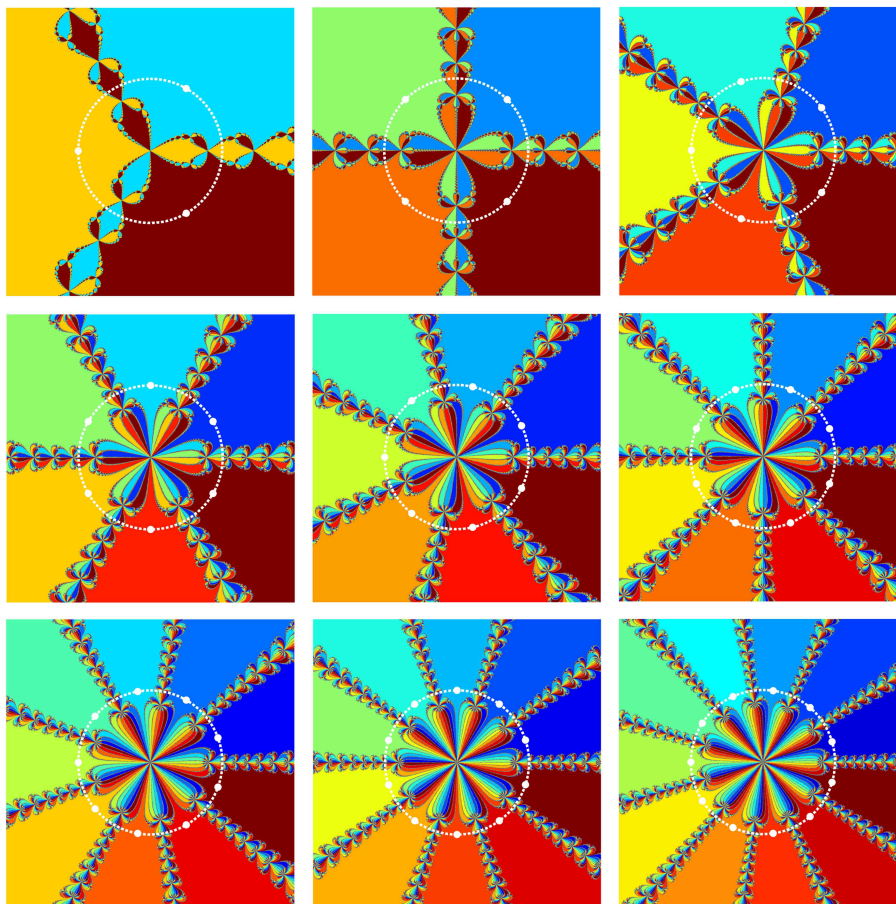
Figure 4. Basins of attraction obtained numerically by iterating Eq. (4) on the domain of initial conditions $-2.0 \leq x_0 \leq 2.0$ and $-2.0 - \delta \leq y_0 \leq 2.0 - \delta$ (for $\delta = \sqrt{2}/100$) when $N = 3, 4, 5$ (top row, left to right) $N = 6, 7, 8$ (middle row, left to right), and $N = 9, 10, 11$ (bottom row, left to right).

equilateral triangle on whose vertices the roots sit is rotated by $\pi/3$ radians about the origin, and hence the basins must also be rotated through the same angle.

The Nth Roots of -1

Having glimpsed some of the complexity hiding inside the cube roots of -1, a natural generalization is the Nth *roots of* -1 class of problem, where $N > 3$. The polynomial equation to solve is then $f_N(z) := z^N + 1 = 0$. Since the derivative is $f'_N(z) := \mathrm{d}f_N/\mathrm{d}z = Nz^{N-1}$, the N-R formula becomes a slightly more involved version of Eq. (3):

$$z_{n+1} = z_n - \frac{z_n^N + 1}{Nz_n^{N-1}}. \tag{4}$$

The calculations shown in Fig. 4 are performed on a square grid of 2048×2048 points linearly spaced across the domain Σ of initial conditions $-2.0 \leq x_0 \leq 2.0$

Figure 5. Magnification of the basins of attraction around the tips of a petal region ($0.7 \leq x_0 \leq 1.1$ and $-0.2 \leq y_0 \leq 0.2$) for $N = 7$ (left), $N = 9$ (middle), and $N = 11$ (right) using a 2048×2048 grid with linearly-spaced points. The dashed white lines are arcs of the unit circles shown in the corresponding panes of Fig. 4.

and $-2.0 - \delta \leq y_0 \leq 2.0 - \delta$).[1] The iterates are assumed to have converged when $|z_{n+1} - z_n| \leq 10^{-8}$, and the total number of iterations allowed for any particular z_0 before assuming non-convergence is chosen to be 10^6. For each z_0, the value of $\lim_{n\to\infty} z_n$ is interrogated; its argument is used to find the final angular position in the Argand plane (and hence identify the root onto which the trajectory has converged), its magnitude checked to make sure $|\lim_{n\to\infty} z_n| \approx 1$, and then a corresponding color assigned. As a global observation, for increasing N we see that the central portion of the basins pattern develops a petal-like structure with much intricate self-similar detail (see Fig. 5).

Uncertainty dimension

In the preceding section, we saw that the N-R method in combination with solving $f_N(z) = 0$ provides a simple iterative scheme for generating endlessly fascinating structures. Inspection of Figs. 4 and 5 strongly suggest that these patterns exhibit a level of self-similarity, and they provide some anecdotal evidence supporting the conjecture that their mathematical nature might be bound up with multiscaled-ness. But saying something "looks fractal" is not really very scientific. Ideally, we want to find a way of quantifying consistently the level of fractality so as to compare different patterns in a meaningful way.

At this juncture, one is obliged to introduce the concept of *fractal dimension* [8] with an objective, broadly speaking, of translating the qualitative degree-of-complexity into a numerical value. There are many different definitions of fractal dimension—each with its own very specific algorithm—and a key sticking point is that not all such yardsticks may be applied in all cases. Here, we will consider only the *uncertainty dimension* [9]. It has an elegant and clear-cut interpretation that is readily understandable in physical terms and appeals to one's intuition about classical cause-and-effect relationships in general.

Estimating the uncertainty dimension D, where $1 < D \leq 2$, involves a prescription for assigning to a dynamical system a number that is tightly connected to the susceptibility of that system's long-term output (namely $\lim_{n\to\infty} z_n$) to small fluctuations at its input. Each point on the (x_0, y_0) grid is subjected to a simple test by

---

[1] Offsetting the grid by a small number in this way, e.g. with $\delta = \sqrt{2}/100$, has the desirable effect of suppressing initial conditions that lie on the lines $x_0 = y_0$ and $x_0 = -y_0$, which otherwise often lead to an artificially high number of non-converging trajectories when N is a multiple of 8.
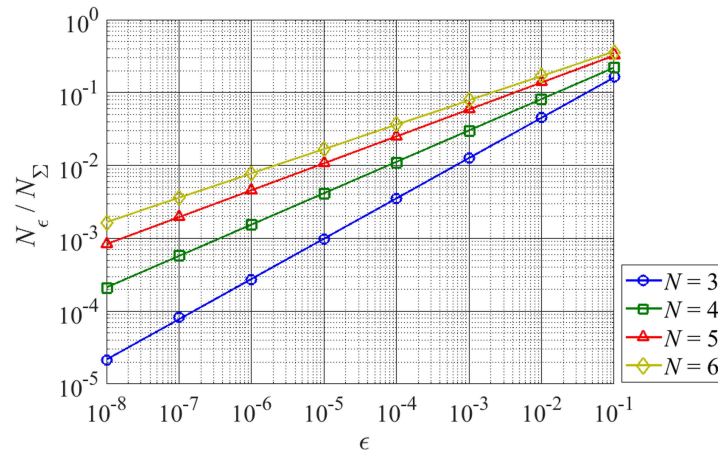
Figure 6. Numerical calculation of the fraction of initial conditions exhibiting final-state sensitivity, N_ϵ/N_Σ, as a function of ϵ for four low-degree polynomials. The domain Σ of the (x_0, y_0) Argand plane considered in each case is identical to that defined in the caption of Fig. 4. The points correspond to raw data, and the best-fit lines (obtained using MATLAB's `polyfit` function) are used to estimate D.

performing computations for a triplet of initial conditions: $(x_0, y_0 - \epsilon)$, (x_0, y_0), and $(x_0, y_0 + \epsilon)$ for a disturbance $0 < \epsilon \ll \mathcal{O}(1)$. If all three of our starting points lead to trajectories converging onto the same attractor, then we say (x_0, y_0) does not exhibit sensitive dependence on initial conditions (that is, the long-term behaviour of the iterates is independent of ϵ). But if the the same attractor is *not* reached in all three cases, we associate (x_0, y_0) with the property of final-state sensitivity (FSS) or, perhaps more famously, *the butterfly effect* [5]: arbitrarily-small fluctuations at the input lead to arbitrarily-large changes at the output. A system exhibiting this property is then classified as being *chaotic*.

For a grid comprising N_Σ points of which N_ϵ test positive for FSS at a given ϵ, we find that $N_\epsilon/N_\Sigma \sim \epsilon^\alpha$. The uncertainty exponent α is here defined to be $\alpha := 2 - D$, where the significance of the factor 2 is that it denotes the topological, or Euclidean, dimension of the space Σ being considered [evidently, that dimension must be 2 for the Nth *roots of* -1 class of problem since we are dealing with the (x_0, y_0) plane]. A back-of-the-envelope calculation shows that D is related to the slope of a log-log graph, typically through

$$D = 2 - \frac{\mathrm{d}\log_{10}(N_\epsilon/N_\Sigma)}{\mathrm{d}[\log_{10}(\epsilon)]}, \tag{5}$$

and where it is now sensible for ϵ to span decimal orders of scale. As the log-log slope tends to zero, $D \to 2$ and the structure of the basin boundaries is expected to become more and more area-filling (with detail packed increasingly tightly into the same space). Thus, D tells us how robust or stable a system is [9]; larger values are associated with greater sensitivity to initial fluctuations and that physical attribute appears as increasing pattern complexity. A selection of log-log plots is shown in Fig. 6 for some low values of N and with ϵ spanning eight decimal orders of scale.

In Fig. 7, we estimate the uncertainty dimension D as a function of N. The curve $D(N)$ does not seem to approach the upper limit of 2, but rather it tends to flatten out towards a limiting value of ≈ 1.8 (at least across the range of N considered here).
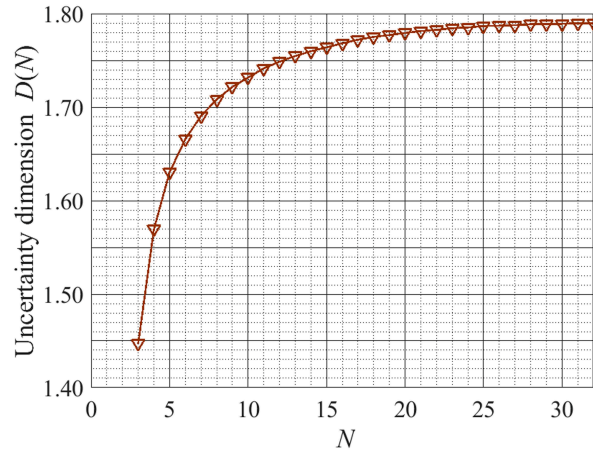
Figure 7. Computed uncertainty dimension D, defined in Eq. (5), as a function of the polynomial degree N for the domain matching that shown in Fig. 4. Almost exactly the same curve is recovered when considering the domain used in Fig. 5.

Somewhat tellingly, the case of $N = 2$ is omitted from these results. That is because the basin boundary in the *square roots of −1* problem is a straight line (see Fig. 1) rather than a self-similar pattern, and so the log-log plot in that case is not especially meaningful.

A curious phenomenon begins to emerge for higher-N polynomials (typically $N \geq 11$), where self-similar distributions of circles appear within the basin boundaries. These circles start off as quite small features, but they gradually grow in size with N (see Fig. 8). It has not been possible to compute long-term trajectories for initial conditions inside those circles: MATLAB returns a NaN ("Not a Number") error, which is usually the signature of arithmetic operations $0/0$ or ∞/∞. It is conceivable that these trajectories 'land on infinity' without being attracted to that point ('infinity' is known to be a repeller for N-R problems involving polynomials of arbitrary degree), or they might return to the vicinity of the roots after orbiting beyond distances that can be handled by MATLAB.

Final state sensitivity in Newton-Raphson

The key ingredient driving FSS is *nonlinearity*. A system can be classified, somewhat generically, as "linear" when *output $\propto$ input*; for instance, $z_{n+1} = \lambda z_n$, where λ is a constant. Nonlinear systems such as Eqs. (1)−(4), by definition, do not satisfy that proportionality. One of the effects of nonlinearity, as we have seen in the previous section, is to magnify the effect of initial fluctuations in quite a dramatic way.

Figure 2 is an illustration of how FSS can appear on computer when solving N-R problems. Mathematically, we *know* that the solution generated by Eq. (2c) *must be indistinguishable* from that obtained by Eq. (1) when $y_0 = 0$; after all,

$$z_{n+1} = z_n - \frac{z_n^2 + 1}{2z_n} = \frac{2z_n^2 - (z_n^2 + 1)}{2z_n} = \frac{z_n^2 - 1}{2z_n}. \qquad (6)$$

The right-hand side is then identical to Eq. (2c) when z_n is replaced by x_n. However, one is obliged to recognize that there is a small but finite difference, computationally
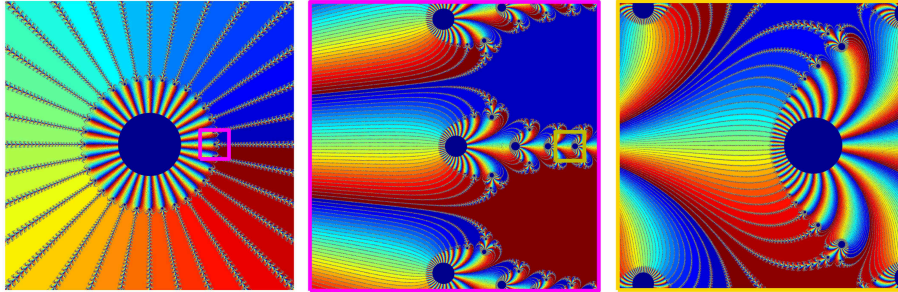
Figure 8. Magnification of the basins of attraction for $N = 32$ across three decimal orders of scale. Left: $-2.0 \leq x_0 \leq 2.0$ and $-2.0 - \delta \leq y_0 \leq 2.0 - \delta$, with $\delta = \sqrt{2}/100$. Middle: $0.7 \leq x_0 \leq 1.1$ and $-0.2 \leq y_0 \leq 0.2$. Right: $1.04 \leq x_0 \leq 1.08$ and $-0.02 \leq y_0 \leq 0.02$. Initial conditions lying in the dark blue circles give rise to numerically indeterminable trajectories in the long term.

speaking, between the two numbers

$$X - \frac{X^2 + 1}{2X} \quad \text{and} \quad \frac{X^2 - 1}{2X}. \tag{7a}$$

That difference is so tiny, so close to zero, as to be almost imperceptible. For instance, when $X = 1.8$ (corresponding to the initial condition in Fig. 2), it is easy to show that

$$\epsilon = \left(1.8 - \frac{1.8^2 + 1}{2 \times 1.8}\right) - \left(\frac{1.8^2 - 1}{2 \times 1.8}\right) \approx 1.1102 \times 10^{-16}. \tag{7b}$$

Under 'normal' circumstances, the fact that ϵ is so small is unimportant and it can be safely neglected. But in the world of nonlinear equations (even just the $N = 2$ case, let alone $N = 3$ or beyond), it can be absolutely essential. When comparing the solutions in Fig. 2, what we are really seeing is an effect mimicking the introduction of tiny fluctuations at the input (strictly, at stage $n = 1$), and which subsequently grow at an incredibly fast rate. Just think for a moment about the numbers involved here: after only 100 iterations of the N-R method, an initial deviation whose magnitude is $\mathcal{O}(10^{-16})$ has grown to dominate the solution [we also note in passing that for the initial condition $(x_0, y_0) = (1.8, 0)$, Eqs. (2a) and (2b) provide a third solution that differs from both those shown in Fig. 2]. That simple result is a prime example of nonlinearity—and the butterfly effect—in action.

Concluding remarks

By starting with a simple root-finding problem, we have seen that the N-R method can give rise to enormous complexity in the Argand plane when seeking iterative solutions to polynomial equations with $N > 2$. While the classic case of cube roots is no doubt well known to many readers, it is hoped that the higher-degree cases briefly discussed here offer something not quite so familiar, and that the estimation of the uncertainty dimension is something new to ponder over and play with. We have also considered the impact of finite computational precision—in essence, "$a - a \neq 0$"—on solving nonlinear equations.

The topic of this article has been something of a center-piece, teaching-wise, in the Physics Department at the University of Salford for the last decade or thereabouts.

As a numerical technique introduced during computing classes, using the N-R method for root-finding can seem rather antiquated: most modern software packages include library routines for solving polynomial equations that yield almost instantaneous answers to incredible accuracy (for instance, the `roots` command in MATLAB). But we believe there is much to be gained from studying simple problems of the type discussed here. What undergraduate student can see the striking patterns generated by Newton-Raphson and not be immediately inspired by the profound beauty of such simple mathematics? The problem has nonlinearity, chaos, and fractals. When we interpret Eqs. (1)−(4) as dynamical systems, we find a seamless merging of mathematics, physics, and computation facilitated entirely by a feedback process that was (quoting from Gleick's gem) "already old when Newton invented it" [5].

Summary. We consider a systematic generalization of the well-known *cube roots of* −1 problem to include the Nth roots. The associated fractal basin boundaries are computed, and we also explore how sensitive this class of systems is to fluctuations at its input by estimating the "uncertainty" fractal dimension. Other curious results are uncovered along the way.

References

1. Alligood, K. T., Sauer, T. D., Yorke, J. A. *Chaos: An Introduction to Dynamical Systems*. Springer, 2009.
2. May, R. M. Simple mathematical models with very complicated dynamics, *Nature* **261** (1976) 459–467.
3. Richter, P. H., Peitgen, H.-O. Morphology of complex boundaries, *Ber. Bunsenges. Phys. Chem.* **89** (1985) 571–588.
4. Initial conditions that result in non-converging trajectories tend to be those lying on (or being very close to) the straight-line geometrical boundaries between the constituent basins of attraction [cf. those shown in Fig. 1 and also Ref. 2].
5. Gleick, J. *Chaos: Making a New Science*. Vintage, 1998.
6. Nusse, H. H., Yorke, J. A. Basins of attraction, *Science* **271** (1996) 1376–1380.
7. Daza, A., Wagemakers, A., Sanjuan, M. A. F., Yorke, J. A. Testing for basins of Wada, *Scientific Reports* **5** (2015) article no. 16579.
8. Mandelbrot, B. B. *The Fractal Geometry of Nature*. Freeman, 1988.
9. McDonald, S. W., Grebogi, C., Ott, E., Yorke, J. A. Fractal basin boundaries, *Physica D* **17** (1985) 125–153.